CI&CEQ

Available on line at
Association of the Chemical Engineers AChE
www.ache.org.rs/CICEQ

Chemical Industry & Chemical Engineering Quarterly 15 (4) 263–270 (2009) CI&CEQ

SANJA RATKOVIĆ
ERNE KISS
GORAN BOŠKOVIĆ

Faculty of Technology, University of Novi Sad, Novi Sad, Serbia

SCIENTIFIC PAPER

UDC 66.097:661.183.8:546.72/.74

DOI: 10.2298/CICEQ0904263R

SYNTHESIS OF HIGH-PURITY CARBON NANOTUBES OVER ALUMINA AND SILICA SUPPORTED BIMETALLIC CATALYSTS*

Carbon nanotubes (CNTs) were synthesized by a catalytic chemical vapor deposition method (CCVD) of ethylene over alumina and silica supported bimetallic catalysts based on Fe, Co and Ni. The catalysts were prepared by a precipitation method, calcined at 600 °C and in situ reduced in hydrogen flow at 700 °C. The CNTs growth was carried out by a flow the mixture of C_2H_4 and nitrogen over the catalyst powder in a horizontal oven. The structure and morphology of as-synthesized CNTs were characterized using SEM. The as-synthesized nanotubes were purified by acid and basic treatments in order to remove impurities such as amorphous carbon, graphite nanoparticles and metal catalysts. XRD and DTA/TG analyses showed that the amounts of by-products in the purified CNTs samples were reduced significantly. According to the observed results, ethylene is an active carbon source for growing high-density CNTs with high yield but more on alumina-supported catalysts than on their silica-supported counterparts. The last might be explained by SMSI formed in the case of alumina-supported catalysts, resulting in higher active phase dispersion.

Key words: carbon nanotubes; bimetallic catalysts; ethylene; catalytic chemical vapor deposition.

Carbon nanotubes (CNTs) are one-dimensional nanostructures with unique mechanical and electrical properties that make them attractive systems for fundamental scientific studies as well as for a wide range of applications [1-3]. Since their discovery by Iijima in 1991 [4], CNTs have become one of the most interesting fields of nanoscience and nanotechnology. Several techniques, such as electric arc-discharge, laser evaporation and catalytic chemical vapor deposition of hydrocarbons (CCVD) have been successfully developed to synthesize carbon nanotubes [5]. The first two methods are not preferred due to their complexity, low selectivity, difficult separation and consequently low yield of CNTs. In this respect, a CCVD technique, allowing control of the size and specific properties of CNTs, seems to be a promising way for the production of large amounts of CNTs under mild conditions [6]. In such a process different hydrocarbons (methane, ethylene, acetylene, benzene or toluene) [7] are flowed over a supported metal (Fe, Co or Ni) catalyst with surface offering a suitable spot for the carbon nanotubes growth [8]. The nanostructure morphology depends on various parameters, associated with a chemical character of the carbon source, catalyst properties and reaction conditions. Thus, almost inert methane and carbon monoxide are claimed to give single-wall carbon nanotubes (SWCNTs) [9-11], whereas more reactive unsaturated hydrocarbons are typically used for muli-wall nanotube growth (MWCNTs) [12-14]. Type of support and its pore size, nature and loading of applied metal and the size of active phase particles are the most important catalyst related properties [15], while temperature, duration of synthesis and space velocity of gas are leading synthesis parameters [16].

In almost two decades of CCVD method development, a lot of efforts have been focused on the catalyst design, comprising both an active phase and support investigations. Thus Fe, Co and Ni have been broadly claimed as metals creating the best active phases [6,13,14], while both traditional [7] and novel supports such as zeolites, $CaCO_3$ and magnesia

Corresponding author: G. Bošković, Faculty of Technology, University of Novi Sad, Bul. Cara Lazara 1, 21000 Novi Sad, Serbia.
E-mail: boskovic@uns.ns.ac.rs
Paper received: 23 July, 2009.
Paper revised: 14 October, 2009.
Paper accepted: 24 October, 2009.
*A part of this study was presented as a poster at the 8th Symposium „Novel Technologies and Economics Development“, University of Niš, Faculty of Technology, Leskovac, October 21-24, 2009.

[7,17,18] have been successfully applied. For example, $CaCO_3$ supported Fe, Co catalyst has been reported as being very effective for MWCNTs production using acetylene as a carbon source [17]. Coexistence of CaO alongside with $CaCO_3$ is the result of partial thermal decomposition of the former at MWCNTs synthesis temperature, leading to two groups of the product differing in their diameter. Using magnesia as a support the same authors have correlated the catalyst and CNTs morphology as a function of the reaction temperature [18]. A direct relationship between the diameter of metal nanoparticles and carbon nanotubes was reported [18], which have also been revealed by other authors [5-7].

Various mechanisms for carbon nanotubes nucleation and growth by CCVD method have been proposed [19]. According to some authors [20,21], carbon nanotubes can exhibit two different synthesis modes during the growth process. When an active metal nanoparticle remains anchored to the surface of support, the synthesis mode is called “base growth”. The growth follows a “tip growth” mechanism when the particle lifts off from the support by the growing C-filament and is observed on the top of the formed CNTs. The difference in growth modes is often explained in terms of adhesion force between the catalyst active metal particle and the support [22].

The purification of synthesized carbon nanotubes is a very important part of the carbon nanotubes production and involves separation and removal of the catalyst and amorphous carbon. The main goal of the process is removal of all impurities from the raw materials without damaging the nanotubes. Despite the significant amount of the research, a large scale synthesis of carbon nanotubes with high purity has not yet reached a maturity level and is under an extensive investigation [23-26].

The role of the catalyst support and a metal active phase in the growth of carbon nanotubes is in the center of the present investigation. For this purpose, different bimetallic catalysts, supported on both silica and alumina, were prepared. Using different methods physicochemical properties of the catalysts are investigated and correlated with an activity in the CNTs synthesis.

EXPERIMENTAL

Catalyst synthesis

Bimetallic catalysts supported on commercial SiO_2 (Kieselgur, Kemika, Zagreb) and γ-Al_2O_3 (Alumina pellets 000-3p, Ketjen Catalysts) were prepared by precipitation of equivalent masses of various pairs of metal hydroxides, keeping the total metal loading of 5 wt.%. The catalyst preparation procedure was as follows: aqueous solutions of $Fe(NO_3)_3{\cdot}9H_2O$, $Co(NO_3)_2{\cdot}6H_2O$ or $Ni(NO_3)_2{\cdot}6H_2O$ were mixed with γ-Al_2O_3 or SiO_2 powder and stirred for 2h at room temperature. By adding the ammonia solution (pH 8) metal hydroxides were precipitated onto the appropriate support. After filtration and washing, the samples were dried at 110 °C for 24 h, then calcinated in air at 600 °C for 5 h. Catalyst precursors in its oxide form were crushed and kept in a closed flask.

Carbon nanotubes synthesis and purification

The carbon nanotubes growth was carried out at atmospheric pressure in a horizontal quartz tube with an external diameter of 42 mm and a length of 1 m. The tube is inside a horizontal electrical furnace controlled by Eurotherm 2204e temperature controller and a K-type TC positioned directly on the quartz tube wall. The system is equipped with a MKS PR 4000 mass flow controller allowing a precise flow of gas mixtures. The catalyst precursor powder (700 mg) was placed in the form of a thin layer in a quartz boat located in the middle of the quartz tube. Prior to the reaction, the catalyst was reduced in the hydrogen flow (110 ml/min) at 700 °C for 2 h. Subsequently, the hydrogen was replaced by the 220 ml/min flow of mixture of ethylene/nitrogen (1:1) and the synthesis was carried out at the same temperature for 1 h. After cooling the system, the catalyst loading together with an accumulated C-containing material were discharged and measured, which was followed by the calculation of the carbon yield according to the formula:

$$\text{Carbon yield} = 100\frac{m_{\text{tot.}} - m_{\text{red.cat.}}}{m_{\text{red.cat.}}}$$

where $m_{\text{tot.}}$ is the total weight of the catalyst and as-synthesized C-containing products and $m_{\text{red.cat.}}$ is the weight of the reduced catalyst which was measured in a separate experiment.

After the synthesis, the raw products were treated with 1 M NaOH solution at 80 °C for 2 h in order to remove the catalyst support. The resulting material was washed several times with distilled water and then treated with 1 M HCl solution in order to remove the remaining metal particles. Subsequently, the purified carbon nanotubes (CNTs) were washed with distilled water and dried at 110 °C for 24 h.

Characterisation of the catalyst and products

The catalysts samples were analyzed both before and after the reaction by XRD using a Powder diffractometer (Seifert MZIV) with CuKα radiation (λ =

= 0.15406 nm). The structure and the morphology of the as-synthesized and purified carbon nanotubes were characterized by the scanning electron microscope (SEM JEOL JSM-6460LV) with an additional quantitative analysis by Energy Dispersive Spectroscopy (EDS). A thermal analysis was used to study the thermal behavior of as-synthesized and purified carbon nanotubes and to determine their purity. DTA and TGA were performed simultaneously in the static air atmosphere from 25 to 1000 °C at ramping rate of 10 °C/min using Derivatograph MOM-1.

RESULTS AND DISCUSSION

Carbon yield

The activities of different bimetallic catalysts in respect to CNTs growth from ethylene are given in Table 1 as the percentage of the carbon yield. As mentioned before, the structure and the morphology of as-synthesized carbon nanotubes depend on the type of the catalyst support and active phase, the method of the catalyst preparation as well as the reaction conditions. It is well known that a number of oxides and mixed oxides have been used to disperse and stabilize small metallic particles [8]. That depends upon the metal-support interactions (MSI) which optimum assures good catalytic properties [27]. According to the results from Table 1, it can be observed that the carbon yield depends on the type of the active phase, as well as on the nature of the catalyst support. All alumina supported bimetallic catalysts showed higher activity in the carbon nanotubes production in comparison to the silica supported ones. It is well established [8] that one of the major factors influencing the catalytic activity is the size of metallic particles substantially determined by the nature of the support and related intensities of the established MSI. In the case of Co, different reducibility has been reported on silica and alumina, the last being characterized with stronger MSI, limited particles mobility, lower chances for their agglomeration and consequently smaller particles size [27]. It might be that in the particular case of bimetallic catalysts present here the same SMSI might be responsible for the higher metal dispersion in the case of alumina supported catalysts resulting in a higher carbon yield.

Concerning different active phases the following activity decline can be observed: Fe,Co > Fe,Ni > > Co,Ni. The carbon yield for the Fe,Co/γ-Al_2O_3 bimetallic catalyst was remarkably high (263.6%), while for the Co,Ni/SiO_2 was the lowest (9.1%). Willems *et al.* [5] showed that cobalt as a catalyst active phase is of the prime importance for obtaining the high quality multi-wall carbon nanotubes, while the use of iron alone can give a higher carbon yield, but the product of lower quality. Thus, the mixture of cobalt with other transitions metals could combine these two advantages and lead to a very high activity in the formation of MWCNTs of good quality. According to Kónya *et al.* [28] the usage of Fe, Co bimetallic catalyst for carbon nanotubes production results in alloy phase formation which is supposed to be the catalytic active phase. The relatively high yield and excellent quality of carbon nanotubes have been explained by the peculiar behavior of this alloy phase [7]. It has been also found that the presence of Co in Fe enhances the bond rearrangement of both carbon and transition metal atoms for easier carbon absorption, diffusion and orientation of tubular C_6 rings into the nanotube structures [18].

Table 1. Carbon yield by ethylene decomposition over different bimetallic catalysts (calculated as % of accumulated carbon relative to the mass of catalyst used in its reduced form)

Catalyst	Carbon yield, %
Fe,Ni/γ-Al_2O_3	239.1
Fe,Co/γ-Al_2O_3	263.6
Co,Ni/γ-Al_2O_3	76.4
Fe,Ni/SiO_2	47.3
Fe,Co/SiO_2	61.8
Co,Ni/SiO_2	9.1

SEM characterization

The morphology of the as-synthesized carbon nanotubes located on the top of different catalysts is presented by SEM images in Figs. 1a-1f. It has to be mentioned that due to the limitation of the SEM technique, a tubular shape of the obtained C-containing nanostructures cannot be certainly proven. However, the C-source and the reaction conditions applied guarantee the CNTs structure of the product [22]. As it can be seen, different catalyst active phases and supports result in CNTs of different morphology. SEM images revealed the high selectivity of the carbon nanotubes formation over alumina-based catalysts leading to a homogeneous and dense distribution of CNTs covering the catalyst surface in a web-like network (Figs. 1d-1f). In contrast, the density of CNTs grown over silica-supported catalysts was lower (Figs. 1a-1c; notice different magnification applied). This suggests that the catalysts prepared on silica lack homogeneity of its active phase being responsible for CNTs growth. An extreme example is the Co,Ni/SiO_2 sample, with the surface covered only with traces of C-containing forms (Fig. 1c). According to the SEM images, carbon nanotubes synthesized over present bimetallic cata-

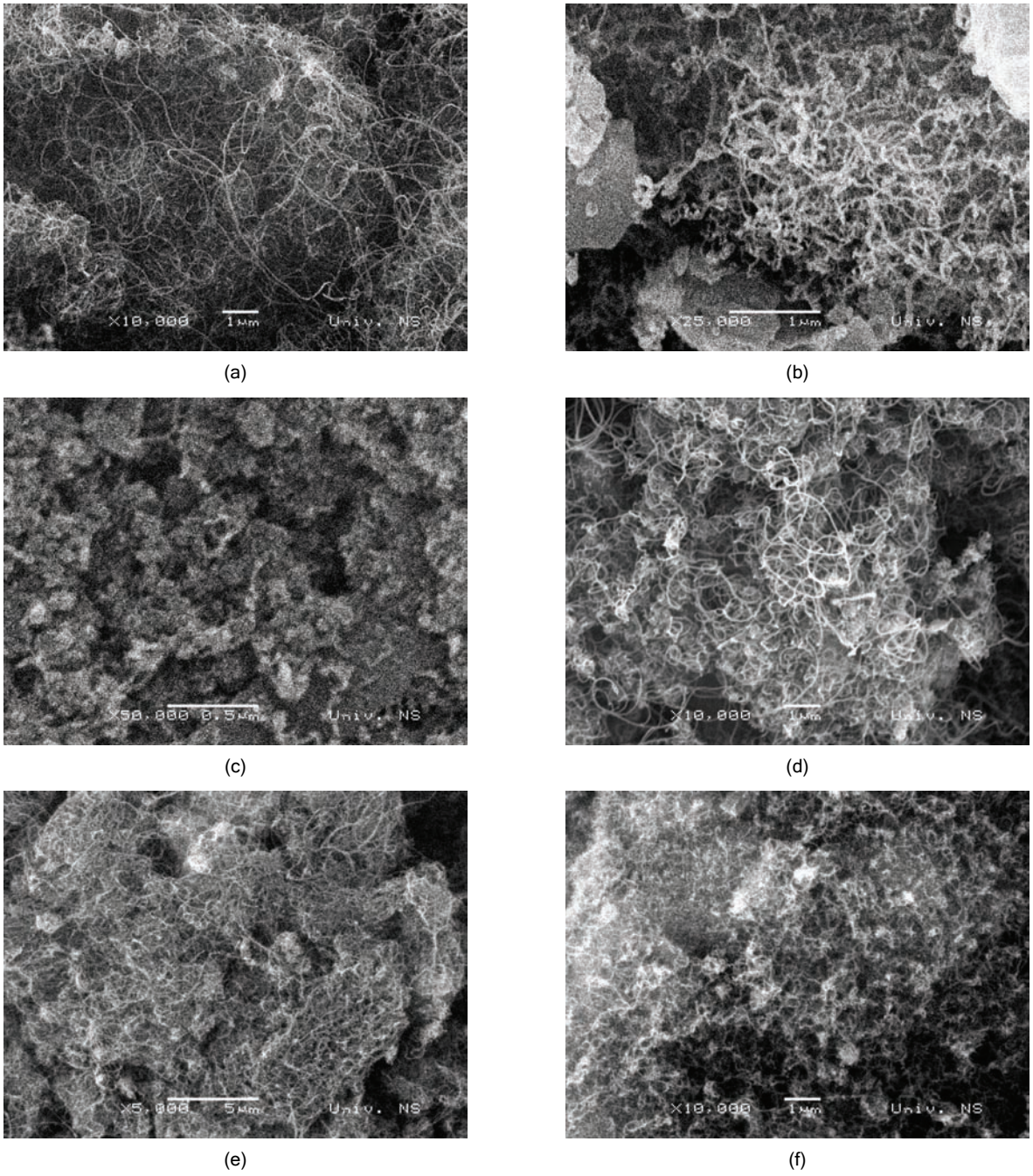

Figure 1. SEM images of the CNTs grown over a) Fe,Co/SiO_2; b) Fe,Ni/SiO_2; c) Co,Ni/SiO_2; d) Fe,Ni/γ-Al_2O_3; e) Fe,Co/γ-Al_2O_3; f) Co,Ni/γ-Al_2O_3 bimetallic catalysts in the flow of ethylene and nitrogen mixture (110/110 ml/min) at 700 °C for 1 h.

lysts are very tangle indicating the presence of structural defects responsible for twisting of the tubes [23]. All the CNTs grown over particular bimetallic catalysts have diameters in the range of 20-60 nm. However, due to the limited number of pictures taken at higher magnification it was not possible to narrow the estimation of the exact thickness of the nanotubes and connect that to either particular active phase or to the support. It is known that in the CCVD method the diameter of as-synthesized CNTs is almost equal to that of the catalyst particles [29,30].

Thus, it can be suggested that the diameters of all catalyst particles were in the same range, speaking on not very uniform dispersion achieved among different catalytic systems, as well as within a single catalyst sample. It was reported [31] that an optimized catalyst particle size allows a good balance between the rates of hydrocarbon decomposition and carbon filament growth. Also, the good balance between these

two rates enables the selective growth of carbon nanotubes and prevents the formation of amorphous carbon which leads to deactivation of the catalysts and completion of CNTs growth.

An additional peculiar structure of the obtained CNTs is connected to the particular most active Fe, Co catalyst having CNTs of very high density. Namely, as shown in Fig. 2 some parts of the catalyst surface is covered with the as-grown CNTs in the form of quasi-aligned bundles. SEM image obtained with higher magnification (Fig. 2b) shows one of these bundles, witnessing its extremely high density which might be the reason for the highest carbon yield achieved with the particular catalyst. As it can be seen, the as-grown CNTs bundle has the diameter in the range of 3-5 μm and consists of densely packed nanotubes which are almost parallel to each other along the direction of the bundle axis. It has to be mentioned, however, that the organization of nanotubes in bundles is connected exclusively to the present alumina-supported Fe, Co catalyst. It is known that single-wall nanotubes (SWNTs) are usually assembled into macroscopic bundles by van der Waals interactions [32-35], whereas multi-wall carbon nanotubes (MWNTs) generally come either as disordered individual tubes or aligned CNTs array [36]. Although the presence of MWNTs in bundles has been reported occasionally [37,38], the bundles growth mechanism is still an open question. According to Mukhopadhyay [39], the presence of Fe coupled with Co could be responsible for the quasi-alignment of CNTs and formation of bundles.

Purification efficiency

In order to obtain the high-purity CNTs, the as-grown nanotube samples were purified by the method of "liquid oxidation" [24] which implies the basic and acid treatment of the raw CNTs material. Figure 3 represents the SEM images of both unpurified and purified CNTs synthesized over Fe,Co/γ-Al_2O_3 bimetallic catalyst, as well as the EDS spectrums of the same samples. As it can be seen from the above SEM images, the CNTs are in the form of highly interwoven structures which were not disturbed by the applied purification process. Due to low magnification of the applied SEM equipment, catalyst metal particles can be observed in neither of the figures. However, the results from corresponded EDS spectra convince that the applied purification method, although not fully accomplished when catalyst removal is concerned, is well chosen. Thus, the weight percentage of carbon and aluminum are 81.3 and 6.2% *vs.* 86.9 and 1.5% in unpurified and purified sample, respectively.

XRD characterisation

Figure 4 shows the XRD patterns for alumina support, Fe,Co/γ-Al_2O_3 catalyst after the calcination and the reduction, as well as patterns of unpurified and purified carbon nanotubes obtained by using the same catalyst. According to Figs. 4a-4c, the XRD spectrums of the catalyst after the calcination and reduction are very similar to the spectrum of pure γ-alumina. This is due to the presence of metals of low concentration in the catalyst which therefore cannot be detected by XRD. The peak at 2θ = 46.5° which corresponds to γ-alumina is present in all the diffractograms; however its intensity decreases upon CNTs formation (Fig. 4d), and almost disappears after CNTs purification (Fig. 4e). At the same time the intensities of XRD lines at 2θ = 26.5° and 2θ = 43.5°, which respectively were assigned to graphite-like phase with (002) and (100) diffraction planes [40], both increased. These results are in line with those obtained by EDS (Fig. 3), speaking on effectively performed CNTs

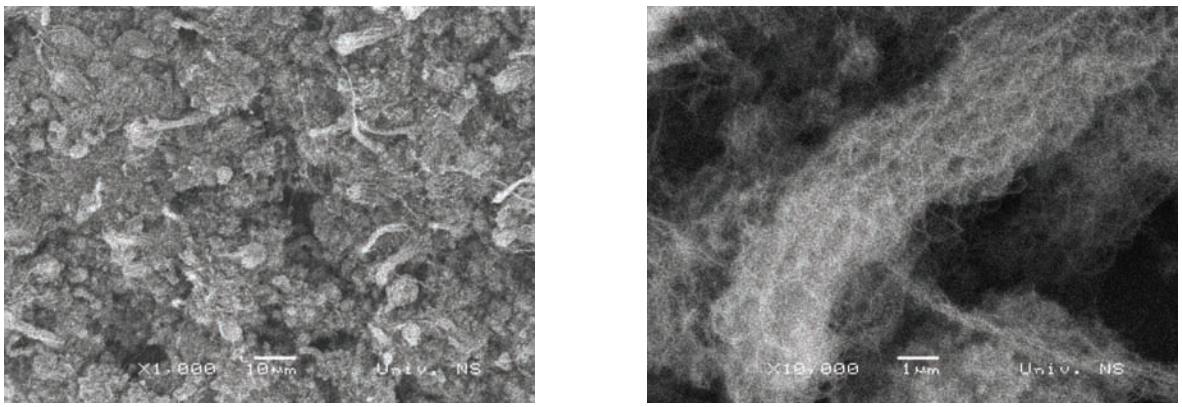

(a) (b)

Figure 2. SEM images of lower a) and higher b) magnification of quasi-aligned CNTs bundles synthesized over Fe,Co/γ-Al_2O_3 catalyst in the flow of ethylene and nitrogen mixture (110/110 ml/min) at 700 °C for 1 h.

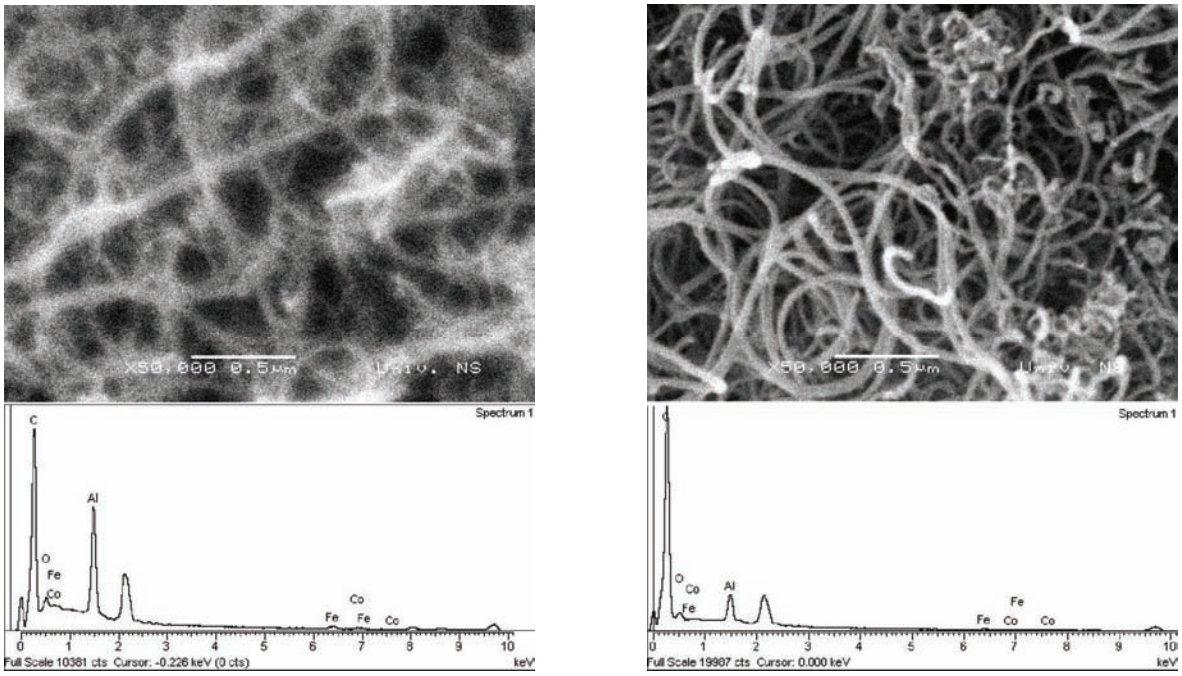

(a) (b)

Figure 3. SEM images and corresponding EDS spectra of both a) unpurified and b) purified CNTs synthesized over Fe,Co/γ-Al_2O_3 catalysts in the flow of ethylene and nitrogen mixture (110/110 ml/min) at 700 °C for 1 h.

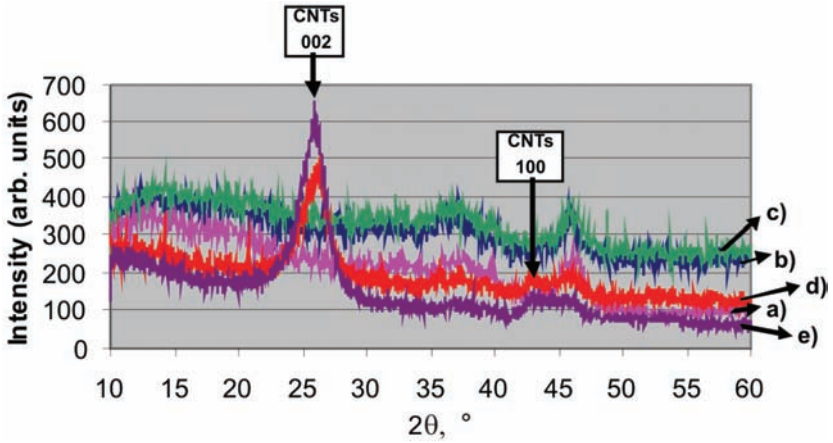

Figure 4. XRD patterns for a) γ-Al_2O_3; b) Fe,Co/γ-Al_2O_3 catalyst after the calcination; c) Fe,Co/γ-Al_2O_3 catalyst after the reduction; d) unpurified and e) purified CNTs synthesized over Fe,Co/γ-Al_2O_3 catalyst in the flow of ethylene and nitrogen mixture (110/110 ml/min) at 700 °C for 1 h.

purification. The main features of X-ray diffraction pattern of as-grown CNTs (Fig. 4d) are close to those of graphite and are principally represented by (002) peak at $2\theta = 26.5°$ [40]. XRD has been proven to be a useful tool for characterizing the alignment of CNTs by checking the intensity of (002) peak at $2\theta = 26.5°$. In particular, the intensity of this peak decreases considerably with higher nanotube alignment [41]. Thus, the intensity increase of the (002) line upon CNTs purification (Figs. 4d-4e) indicates that as-grown CNTs, which are very interlinked staying on the top of the catalyst surface, become even more twisted once they are freed from its catalyst host. This is in accordance with the SEM results given in Figs. 3a and 3b. On the other hand, the shape of the peak for the (002) line (its height and narrowness) can be connected to the C-containing sample graphitization and crystallization degree [41]. Thus, the narrow shape of the peak corresponding to (002) crystal plane of the purified sample (Fig. 4e) suggests its higher graphitization and crystallization degree, which might be the consequence of the removal of amorphous carbon from the outer walls of the tubes. However, this assumption has to be confirmed by TEM technique.

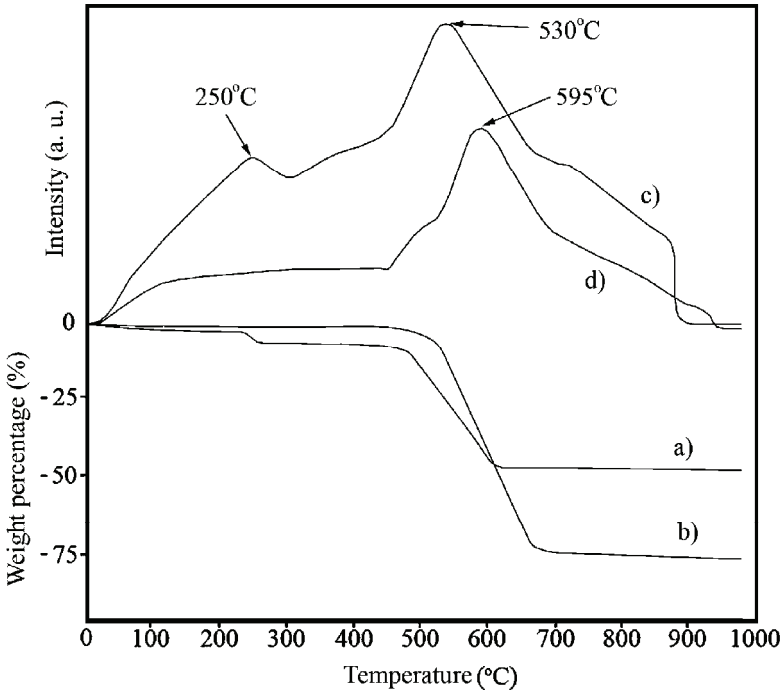

Figure 5. TGA and DTA curves of unpurified (a, c) and purified (b, d) CNTs synthesized over Fe,Co/γ-Al_2O_3 catalyst in the flow of ethylene and nitrogen mixture (110/110 ml/min) at 700 °C for 1 h.

DTA/TGA characterization

Figure 5 shows TGA and DTA curves of unpurified (a, c) and purified (b, d) CNTs synthesized over Fe,Co/γ-Al_2O_3 catalyst in the flow of ethylene and nitrogen mixture (110/110 ml/min) at 700 °C for 1 h. From the TGA and DTA profiles it can be observed that thermal properties of C-containing material largely depend upon the type of carbon present. Namely, as it can be seen from the DTA of an unpurified sample (line c in Fig. 5) CNTs tend to oxidize at higher temperatures than amorphous carbon due to a smaller number of active sites available for oxidation [42]. The same can be followed by TGA, the weight loss profile of the same sample being characterized with two weight loss regions (line a in Fig. 5). The first weight loss around 250 °C contributes to 5% of the total weight loss and can be attributed to the oxidation of amorphous carbon [17,18,42]. The mass drop at 530 °C amounting to 49% of the total weight loss is due to CNTs combustion [17].

DTA and TGA curves of the purified CNTs sample verify the efficiency of the used purification method. The single DTA peak in the high temperature region along with the corresponding weight loss of 75% in TGA (lines d and b) speaks on substantial reduced amounts of both amorphous carbon and catalyst remains after purification. Namely, somewhat lower oxidation temperature of as-synthesized CNTs is usually reported in the literature as a consequence of an additional catalytic effect occurring during thermal oxidation [42].

CONCLUSIONS

In summary, ethylene diluted with nitrogen seems to be an appropriate C-source for growing carbon nanotubes over different bimetallic catalysts using CCVD method at temperature of 700 °C. The higher yield of carbon nanotubes synthesized over alumina-supported catalysts in comparison to the silica-supported counterparts may be the consequence of SMSI occurring in the case of the first support, resulting in higher active phase dispersion and active sites accessibility. According to the results shown in this paper, it can be suggested that "liquid oxidation" purification method can be applied for obtaining high-purity CNTs. It has to be underlined, however, that deeper insight into different support contribution to the catalysts activity, a mechanism of CNTs growth, as well as C-containing product structure cannot be performed without further investigation by TEM, HR-TEM or Raman spectroscopy.

Acknowledgments

Financial support of the Ministry of Science and Technological Development of Serbia (Project 142024, "To Green Chemistry *via* Catalysis") is highly appreciated.

REFERENCES

[1] S.S. Fan, M.G. Chapline, N.R. Franklin, T.W. Tombler, A.M. Cassell, H. Dai, Science **283** (1999) 512

[2] P.M. Ajayan, Chem. Rev. **99** (1999) 1787

[3] J. Cumings, A. Zettl, Science **289** (2000) 602

[4] S. Iijima, Nature **354** (1991) 56

[5] I. Willems, Z. Kónya, J.-F. Colomer, G. Van Tendeloo, N. Nagaraju, A. Fonseca, J. B. Nagy, Chem. Phys. Lett. **317** (2000) 71

[6] A.K.M. Fazle Kibria, Y.H. Mo, K.S. Nahm, M.J. Kim, Carbon **40** (2002) 1241

[7] K. Hernadi, Z. Kónya, A. Siska, J. Kiss, A. Oszkó, J. B. Nagy, I. Kiricsi, Mater. Chem. Phys. **77** (2002) 536

[8] N. Nagaraju, A. Fonseca, Z. Kónya, J. B. Nagy, J. Mol. Catal. A **181** (2002) 57

[9] B. Kitiyanan, W.E. Alvarez, J.H. Harwell, D.E. Resasco, Chem. Phys. Lett. **317** (2000) 497

[10] W.E. Alvarez, B. Kitiyanan, A. Borgna, D.E. Resasco, Carbon **39** (2001) 547

[11] J.E. Herrera, L. Balzano, A. Borgna, W.E. Alvarez, D.E. Resasco, J. Catal. **204** (2001) 129

[12] H.J. Dai, J. Kong, C.W. Zhou, N. Franklin, T. Tombler, A. Cassel, S.S. Fan, M. Chapline, J. Phys. Chem. B **103** (1999) 11246

[13] P. Piedigrosso, Z. Konya, J.F. Colomer, A. Fonseca, G. Van Tendeloo, J.B. Nagy, Phys. Chem. Chem. Phys. **2** (2000) 163

[14] A. Kukovecz, Z. Konya, N. Nagaraju, I. Willems, A. Tamasi, A. Fonseca, J.B. Nagy, I. Kiricsi, Phys. Chem. Chem. Phys. **2** (2000) 3071

[15] A. Gohier, C.P. Ewels, T.M. Minea, M.A. Djouadi, Carbon **46** (2008) 1331

[16] A. Fonseca, K. Hernadi, P. Piedigrosso, J.F. Colomer, K. Mukhopadhyay, R. Doome, S. Lazarescu, L.P. Biro, Ph. Lambin, P.A. Thiry, D. Bernaerts, J.B. Nagy, Appl. Phys. A **67** (1998) 11

[17] E. Dervishi, Z. Li, A.R. Biris, D. Lupu, S. Trigwell, A.S. Biris, Chem. Mater. **19** (2007) 179

[18] E. Dervishi, Z. Li, F. Watanabe, Y. Xu, V. Saini, A.R. Biris, A. S. Biris, J. Mater. Chem. **19** (2009) 3004

[19] Ch. Laurent, E. Flahaut, A. Peigney, A. Rousset, New J. Chem. **22** (1998) 1229

[20] I. Song, Y. Cho, G. Choi, J. Park, D. Kim, Diamond Relat. Mater. **13** (2004) 1210

[21] C. Bower, O. Zhou, W. Zhu, D. Werder, S. Jin, Appl. Phys. Lett. **77** (2000) 2767

[22] K.B.K. Teo, C. Singh, M. Chowalla, W.I. Milne, Catalytic Synthesis of Carbon Nanotubes, Nanofibres, in: Encyclopedia of Nanoscience and Technology, Vol. 1, H.S. Nalwa, Ed., 2004.

[23] B. Louis, G. Gulino, R. Vieira, J. Amadou, T. Dintzer, S. Galvagno, G. Centi, M.J. Ledoux, C. Pham-Huu, Catal. Today **102-103** (2005) 23

[24] A.G. Rinzler, J. Liu, H. Dai, C.B. Huffman, F.J. Rodriguez-Macias, P.J. Boul, Appl. Phys. A **67** (1998) 29

[25] G.S. Duesberg, W. Blau, H.J. Byrne, J. Muster, M. Burghard, S. Roth, Synth. Met. **103** (1999) 2484

[26] M. Holzinge, A. Hirsch, P. Bernier, G.S. Duesberg, M. Burghard, Appl. Phys. A **70** (2000) 599

[27] G. Bošković, J.S.M. Zadeh, K.J. Smith, Catal. Lett. **39** (1996) 163

[28] Z. Kónya, J. Kiss, A. Oszkó, A. Siska, I. Kiricsi, Phys. Chem. Chem. Phys. **3** (2001) 155

[29] K. Hernadi, A. Fonseca, J.B. Nagy, D. Bernaerts, A.A. Lucas, Carbon **34** (1996) 1249

[30] P. Chen, H.-B. Zhang, G.-D. Lin, Q. Hong, K.R. Tsai, Carbon **35** (1997) 1495

[31] M.A. Ermakova, D. Yu. Ermakov, G.G. Kuvshinov, L.M. Plyasova, J. Catal. **187** (1999) 77

[32] B. Vigolo, A. Penicaud, C. Coulon, C. Sauder, R. Pailler, C. Journet, Science **290** (2000) 1331

[33] K.M. Liewa, C.H. Wong, M.J. Tan, Appl. Phys. Lett. **87** (2005) 1901

[34] Q.H. Yang, S. Bai, T. Fournier, F. Li, G. Wang, H.M. Cheng, J.B. Bai, Chem. Phys. Lett. **370** (2003) 274

[35] M.L. Terranova, S. Orlanducci, E. Fazi, V. Sessa, S. Piccirillo, M. Rossi, D. Manno, A. Serra, Chem. Phys. Lett. **381** (2003) 86

[36] C. Zhu, Z. Xie, K. Guo, Diamond Relat. Mater. **13** (2004) 180

[37] S. Klaus, Carbon **33** (1995) 915

[38] Y. Ning, X. Zhang, Y. Wang, Y. Sun, L. Shen, X. Yang, G. V. Tendeloo, Chem. Phys. Lett. **366** (2002) 555

[39] K. Mukhopadhyay, G.N. Mathur, Int. J. Nanosci. **2** (2003) 153

[40] T. Belin, F. Epron, Mater. Sci. Eng. B **119** (2005) 105

[41] C. Hsieh, Y. Lin, J. Lin, J. Wei, Mater. Chem. Phys **114** (2009) 702

[42] J. Liu, A.T. Harris, Chem. Eng. Sci. **64** (2009) 1511.